Pedochemical characterisation and landscape history of the Thangbi river terrace system, central Bhutan

by

THOMAS CASPARI[a], RUPERT BÄUMLER[a], TSHERING DORJI[b], CHENCHO NORBU[b], KADO TSHERING[b], IAN BAILLIE[b,c]

[a] Lehrstuhl für Bodenkunde, Department für Ökologie, Technische Universität München, 85350 Freising-Weihenstephan, Germany

[b] National Soil Services Centre, Ministry of Agriculture, PO Box 119, Simtokha, Bhutan

[c] National Soil Resources Institute, Cranfield University, UK

with 10 figures and 3 tables

Summary. The properties and development of soils formed on fluvial deposits in the valley of the river Chamkhar Chhu, 10 km north of Jakhar, central Bhutan, were examined.

Fieldwork in 2000 and 2002 revealed a system of at least 28 river terraces rising to relative heights of nearly 300 meters. The largest and still well preserved terrace of the system is of late Pleistocene age. Polygenetic structures & buried topsoils indicate several interruptions of soil development under periglacial conditions. ^{14}C AMS dating suggests discontinuities at approximately 10175, 8710, 4055 and 1715 years BP.

Pedochemical analyses showed that all examined soils are moderately weathered and leached and can mostly be classified as Cambisols. X-ray diffraction analyses of clay fractions revealed that especially on the upper terraces pedogenic chlorite formed at the expense of illite. Weighted profile averages of texture, specific surface area (BET), pedogenic iron compounds and weathering indices show significant trends within the terrace system and indicate that weathering and soil development continuously become more intense with increasing relative height above the current river level.

Zusammenfassung. *Pedochemische Charakterisierung und Landschaftsgeschichte des Flussterrassensystems bei Thangbi, Zentralbhutan.* – In Zentralbhutan, 10 km nördlich von Jakhar, wurden Böden aus fluvialen Ablagerungen untersucht. Ziel war es, sie erstmals ausführlich zu charakterisieren und ihre Entstehung in Bezug zur Landschaftsgeschichte zu erhellen.

Bei Geländearbeiten in den Jahren 2000 und 2002 wurde ein System aus 28 Flussterrassen registriert, das sich bis fast 300 m über dem rezenten Flussniveau erstreckt. Die gut erhaltene Hauptterrasse des Systems ist spätpleistozänen Alters. Der polygenetische Bodenaufbau und fossile A-Horizonte deuten darauf hin, dass die Bodenbildung unter periglazialen Bedingungen mehrfach gestört wurde. Mit Hilfe von Radiokohlenstoffmessungen an organischem Bodenmaterial konnten wir derartige Überprägungen für die Zeiträume um 10175, 8710, 4055 and 1715 Jahre vor heute identifizieren.

Unsere pedochemischen Analysen zeigten, dass es sich meist um mäßig verwitterte Böden handelt, die als Cambisole angesprochen werden können. XRD-Analysen der Tonfraktionen konnten vor allem für den oberen Bereich die Bildung von pedogenem Chlorit aus Illit nachweisen. Profilmittelwerte von Körnung, spezifischer Oberfläche, pedogenen Fe-Oxiden und Verwitterungsindizes zeigen deutliche Trends innerhalb des Terrassensystems auf und belegen, dass der Grad der Verwitterungsintensität und Bodenentwicklung mit ansteigender relativer Höhe über dem Flussniveau nahezu kontinuierlich zunimmt.

Résumé. *Caractérisation pédochimique et l'histoire de la formation du système des terrasses fluviatiles à Thangbi, Bhoutan central.* – A Bhoutan central, nous avons étudié des sols issus des dépôts fluviatiles de la vallée de Chamkhar Chhu située à 10 km au nord de Jakhar. Le but de notre étude est de caractériser, pour la première fois, ces sols et de déterminer l'origine de leur formation en fonction de l'histoire de la formation de la vallée.

Pendant les travaux de terrains, en l'an 2000 et 2002, nous avons noté l'existence de 28 terrasses fluviatiles s'étendant sur environ 300 m de dénivelé. La terrasse principale, datée du tertiaire supérieure, est la mieux conservée. Les sols correspondant montrent une structure polygénique due aux interruptions de leur développement sous conditions périglaciaires. La datation par la méthode du Carbone 14 nous a confirmé ces irrégularités à 10175, 8710, 4055 et 1715 ans avant l'actuel.

Nos analyses pédochimiques ont montré que la plupart des sols sont légèrement érodés ce qui pourrait les classifier dans les cambisols. L'analyse par diffraction de rayons X de la fraction argileuse montre la présence de chlorite issue de l'illite ceci a été surtout observé dans les terrasses supérieures. La moyenne pondérée de la granulométrie, la surface spécifique, les oxydes de fer pédogéniques et les indices d'érosion montrent l'existence de bonnes corrélations au sein des terrasses et indiquent que le taux d'érosion ainsi que celui du développement des sols croient continuellement avec l'altitude.

1. Introduction

The kingdom of Bhutan covers about 46000 km^2 on the steep southern slopes of the eastern Himalayas between latitudes 26°47'N to 28°26'N and longitudes 88°52'E to 92°03'E. In the south, it borders the floodplains of the east Indian states of West Bengal and Assam at approximately 200 m a.s.l.. From there, the tropical foothills rise with steep slopes until less steep, basin-like terrain is reached in most parts of the country. Located at altitudes between 2500 up to 4000 m a.s.l., these inner valleys represent Bhutan's cultural heartland. To the north, the gradient increases again to the east-west aligned main chain of the High Himalaya, which includes peaks of more than 7500 m a.s.l. and also marks the border with neighbouring Tibet (China).

Little is known about the soils of Bhutan. KARAN (1967) established a first classification, highlighting their zonal distribution from north to south. This concept was taken up and expanded by OKAZAKI (1987), who suggested five major soil groups that are vertically distributed according to the altitude. A different approach has been taken by BAILLIE et al. (2003). They associated the different soil types with a newly developed physiographic zonation of Bhutan (NORBU et al. 2003) and stressed the importance of polygenetic regoliths in the recently and currently dynamic landscape.

Our study was initiated to increase the knowledge about nature and properties of "typical" Bhutanese soils. For this purpose, the central district of Bumthang was chosen. It is part of the basin-like structures, which are often filled by river sediments. These alluvial landforms and deposits are of major importance for Bhutan, as they provide much of the best arable land, and form the nuclei of the main areas of cultivation and settlement.

They are also of great importance for Quaternary research. In this paper, we will focus on the effects which various deposits as well as Quaternary climatic and geomorphic changes had on soil development. As about two thirds of the total land area are covered by forest, soil erosion is generally low and conditions for the preservation of late Quaternary features are excellent. However, little Quaternary research has been conducted so far. GANSSER (1983) was the first to give a systematic geological account of the Bhutan Himalaya. In the Khoma Chhu valley, northeast Bhutan, he observed remnants of a covered terminal moraine at 2900 m elevation, and noted striations and other possibly glacial features down to altitudes of about 2600 m a.s.l.. He pointed out that it is difficult to recognise early glacial stages below 3000 m a.s.l., mainly because of the intense summer monsoon on Bhutan's southern slopes. TAKADA (1991) surveyed the Quaternary sediments and fluvial terraces near Wangdue-Phodrang, western Bhutan. Although he identified several terrace levels of up to 110 m above the current river level, he concluded that fluvial terraces and deposits in the intramontane basins of Bhutan are rather less developed compared to Nepal, India and Pakistan. There are certainly no features as substantial as the sediments and terraces around Pokhara and Kathmandu in Nepal (YAMANAKA et al. 1982, YOSHIDA & IGARASHI 1984), the Karewa sediments in the Kashmir valley (PAL & SRIVASTAVA 1982), or the sediments in-filling the dun valleys of the Lesser Himalayas (PRASAD & VERMA 1974, ZÖLLER 2000).

In our research area, the valley of the Chamkhar Chhu, GURUNG (2001) has identified a suite of five (I-V) "glacio-fluvial" terraces by geomorphological examination and ^{14}C dating. According to his findings, the lower terraces (I-III) are of Holocene age, and secondary carbonates from debris flow deposits on top of the highest terrace (V) approximately 70 m above the current river level, were dated to 29940 ± 180 BP. Driftwood in the alluvium of the most prominent terrace of the system, terrace IV at approximately 40 m above the current river level, was dated to 27340 ± 180 BP. Both conventional radiocarbon ages indicate that the sediments were deposited during late Pleistocene, before or at the beginning of the global Last Glacial Maximum (LGM).

In 2000, we discovered a large system of associated river terraces at Thangbi along the Chamkhar Chhu, 10 km north of the area examined by GURUNG (2001), representing a more or less complete Quaternary sequence. This paper elucidates our geomorphological field observations and pedochemical analyses to reconstruct the Quaternary history of the present soil types and landforms. Additional terraces were identified in 2002 within the same valley near Kiki La about 20 km south of the study area, which are 280 m, 305 m, 318 m, 330 m, 345 m, and 364 m above the recent river level. However they were not included in the present study.

2. Study area

The Chamkhar Chhu is one of the main rivers draining Bhutan. Our study area is located at 27°37'N and 90°42'E, at Thangbi about 10 km north of Jakhar dzong, the district administration office of Bumthang, central Bhutan (Fig.1).

Within the generally steep terrain of Bhutan, this area is one of the comparatively flat, basin-like sections, which BAILLIE et al. (2003) classified as "Inner Valley", with straight or concave lower slopes. Within this intramontane basin, the speed of the river is reduced and large volumes of sediments were deposited over long time periods. Within our field area, the present river is at 2655 m a.s.l., and associated terraces rise to at least 266 meters above this level.

Land use ranges from arable (lower terraces) through pasture (middle terraces) to natural blue pine forest (*Pinus wallichiana*), which is used for firewood and timber. Barley, wheat and buckwheat are the staple crops in the cool temperate climate with mean temperatures of 4.0°C in December/January and 17.5°C in June-August. The mean annual rainfall is about 800-1000 mm, of which 75% precipitate during the monsoon, i.e. June-September, mostly as falls of low or moderate intensity (BHUTAN SOIL SURVEY 1998).

According to the most recent geological summary based on the field data of the Geological Surveys of India and Bhutan (BHARGAVA 1995), the site is underlain by rocks of the Thimphu group. This group consists of highly metamorphosed rocks, mainly gneiss, some of which is granitic, with mixed muscovite and biotite micas, plagioclase feldspars and quartz as the main minerals.

The deposits of the studied terrace system consist of well-rounded leucogranite boulders and granitic gneiss having been deposited after long-distance transport. GURUNG (2001) identified gneiss, granite and granitic gneiss as the main country rocks in his field area, a few kilometres to the south of ours.

3 Methods

3.1 Sample material

In autumn 2000, 18 profile pits were sited so as to cover the whole range of the terrace system (Fig. 2). A Garmin GPS was used to confirm the locations. The profiles were described and sampled according to FAO (1990) and the soil colours were determined in field-moist state using the Munsell Soil Color Charts (MUNSELL 1994). Horizon designations were made according to the World Reference Base (WRB 1998).

3.2 Physical and chemical analyses

Bulk samples were collected from 16 of the profiles for each distinguishable horizon, air-dried, hand-crushed and sieved to 2 mm. Replicate core samples ($n = 3$, $V = 100\ cm^3$) were also collected. For the measurement of bulk density, the core samples were dried at 105°C and subsequently weighed.

The pH values were measured in deionised water and 1M KCl at a soil-solution ratio of 1:2.5. For particle size distribution, the samples were pre-treated with H_2O_2 to destroy organic matter. After dispersion by shaking with tetrasodium pyrophosphate ($Na_4P_2O_7$) and ammonium oxalate solution for 16 hours, the sand fractions were separated by wet sieving (2000-630 µm, 630-200 µm and 200-63µm). The fraction <63 µm was freeze-dried, suspended in water and subjected to X-ray attenuation (XRA) measurement (Micromeritics Sedigraph 5100) for determining the amount of silt (63-2 µm) and clay (<2 µm).

Organic carbon (C_{org}) and total nitrogen were measured by dry combustion (975°C) in duplicates, using a Vario EL Elementar analyser (minimum detection levels of 0.4 µg for C and 1.0 µg for N).

Total element contents were measured by neutron activation analysis (NAA) at the University of Missouri, USA. The sample is first made radioactive by bombardment with neutrons, then the radioactive isotopes created are identified and the element concentrations are determined by the gamma-rays they emit. NAA is capable of detecting many elements at extremely low concentrations.

Free Fe compounds (Fe_d) were extracted with dithionite-citrate-bicarbonate (DCB) solution (MEHRA & JACKSON 1960). Non- or poorly crystallised Fe-oxides, hydroxides and associated gels (Fe_o) were leached by acid ammonium oxalate solution (SCHWERTMANN 1964). DCB- and oxalate-soluble Al (Al_d and Al_o) were determined in the same extracts.

Silicate-bond iron was calculated from Fe_{t-d}, and well-crystallised iron oxides as Fe_{d-o}. The quotient of well-crystallised iron oxides and total iron content (Fe_{d-o}/Fe_t) was used as a relative measure for weathering intensity (ARDUINO et al. 1984, 1986).

To further elucidate weathering intensities, the index after PARKER (1970) was applied:

$$\text{Parker index, PI} = \left(\frac{Na_a}{0.35} + \frac{Mg_a}{0.9} + \frac{K_a}{0.25} + \frac{Ca_a}{0.7} \right) * 100$$

where X_a represents the atomic portion of ion X, measured by NAA (0 = PI = 100).

It calculates the loss and subsequent leaching of the main alkali and alkaline earth cations by mineral hydrolysis. The numbers in the denominators represent factors to allow for the strength of the element-oxygen bond in the primary minerals. The index decreases with increasing soil development.

For the determination of the cation exchange capacity (CEC), unbuffered 0.5M NH_4Cl solution was used to extract exchangeable cations from 2.5 g air-dried soil (TRÜBY & ALDINGER 1989) at a soil-solution ratio of 1:20. Concentrations of extracted H^+, Na^+, K^+, Ca^{2+}, Mg^{2+}, Mn^{2+} and Al^{3+} were measured by ICP-OES (Perkin Elmer Optima 3000).

Clay fractions (< 2µm) were separated by sedimentation. The clay mineralogical composition was examined by X-ray diffraction analysis (Philips PW 1830 diffractometer) of oriented preparations after saturation of the clay fraction with Mg^{2+} (at 25°C), employing cobalt-Ka radiation and operating at 35 kV and 35 mA. The samples were irradiated between 2° and 18° at a scanning rate of 0.02° and intervals of 5s.

The surface area of the air-dried fine earth was determined by the N_2-adsorption BET approach (BRUNAUER et al. 1938), using an Quantachrome Autosorb 1 surface area analyser. Prior to the measurements the samples were outgassed under vacuum (40 mbar) at 70°C for 24 hours, and then analysed by multiple-step adsorption of N_2 at 77°K in the relative pressure (p/p_o) range of 0.05 to 0.30.

^{14}C-AMS (accelerator mass spectrometry) measurements of subsoil organic matter were performed at the Leibniz laboratory for radiometric dating and isotope research (Kiel, Germany). Pre-treatments of the samples included extraction by 1% HCl, 1% NaOH and 1% NaOH at 60°C, combustion at 900°C and reduction of the generated CO_2 to graphite.

3.3 Data analysis and statistics

To take into account the varying horizon thickness, weighted means of the analytical parameters were calculated for each profile according to the equation:

$$x_m = \frac{\sum (x_i * d_i)}{\sum d_i}$$

x_m = profile-weighted mean

x_i = parameter x of horizon i

d_i = depth of horizon i

We used the one-tailed Student's *t*-test to detect if correlations were significant at the 0.05 (*), 0.01 (**) or 0.001 (***) probability level.

4. Results and discussion

4.1 Field observations

Our field studies in 2000 and 2002 showed that the Thangbi terrace system consists of at least 28 associated river terraces (Fig. 2). In terms of terrace morphology, it clearly falls into two main sections:

The first comprises terrace 1 up to terrace 7 (T1-T7), and consists of horizontal terraces with clear edges and sharp steps. Little weathered material, including huge blocks stemming from catastrophic floods, can be observed frequently. Relative terrace heights are 4 m, 9 m, 17 m, 27 m, 30 m, 34 m and 41 m, and the land is mainly used for arable farming.

The second part of the system consists of terrace 8 and all terraces upslope (T8-T28). Here, we find inclined terraces with unclear steps and rounded edges. The parent material consists of intensively weathered but highly rounded and clearly alluvial gravels. Pasture and forest are the main land use forms. Relative terrace heights are 57 m, 74 m, 86 m, 94 m, 104 m, 113 m, 118 m, 126 m, 130 m, 136 m, 144 m, 153 m, 160 m, 167 m, 176 m, 191 m, 202 m, 211 m, 222 m, 230 m and 266 m, including additional intermediate sublevels.

This division initially suggests that the sediments forming the lower terraces (T1-T7) were deposited at the end of and after the last main glacial period in this area, and have not since been significantly disrupted by periglacial processes. The highest of these young terraces, T7, is more than 500 m wide and may represent the sediments accumulated during the last main melting period of glaciers in northern Bumthang. All terraces above T7 are older and show clear signs of periglacial processes like solifluction and several generations of re-worked loess covers. This indicates that they were deposited before and overlaid during the last main glacial period in this area.

Table 1 summarises the field descriptions of the profiles T4 and T19 as examples of the soils on the young and the old terraces respectively. Silt and clay contents generally increased with increasing height of the terrace above the current river level. This was accompanied by more strongly developed pedal structures in the upper part of the system.

Fig. 3 depicts the main morphological features of six typical profiles. In general, the older terraces show much deeper B horizons. The soils on the upper terraces also have one or more buried topsoils, manifest as darker colours and lower bulk densities. When soils appear to have developed from different parent materials, they are referred to as “polygenetic”.

The only profiles to show the characteristics of a Bt horizon, are located on the terraces T19 (153 m) and T20 (160 m). In both cases, the Bt occurs beneath a buried A horizon, which indicates a period of pedogenic stability and a long interruption in sedimentation. Increases in clay content with depth appear to be mainly due to the complex histories of alluvial, aeolian and periglacial deposition and not to argilluviation. However, some clay translocation has been noted in similar soils elsewhere in Bhutan (BAILLIE et al. 2003).

4.2 Basic laboratory analyses

Despite these differences in morphology, the laboratory analyses did not reveal major chemical differences between the soils on terraces of different ages, as can be seen in Table 2.

Fig. 4 shows the depth functions of organic matter and base status indicators in the profile of T19, which is typical of most of the soils. The pH values are low throughout, reflecting the felsic origins of the granitic alluvial and gneissic periglacial deposits. All samples were carbonate-free. The organic C profile shows a significant increase at about 3 m, which confirms the field indications of a deeply buried fossil topsoil. At the same depth, the total N profile only shows a minor bulge, possibly because of N losses since burial or because of woody nature of the original litter. Within the terrace system, there is no significant increase of C or N values with increasing height above the current river level. The CEC values are low throughout, mostly below 6 $cmol_c\ kg^{-1}$. This reflects the soil's coarse texture but the values are still low for soils with presumed illitic and micaceous clays and in the horizons with higher clay contents. This points to a dominance of low activity clays. In Fig. 4, the maxima of the CEC profile correspond with those for organic C and confirm the existence of a buried paleosol. The intermediate maximum at approximately 2 m corresponds to increasing clay contents.

Bulk densities were generally low and ranged from 0.8-1.5 $g\ cm^{-3}$. These low values may reflect the aeolian origin of some of the sediments.

Following the WRB (1998) classification, most soils were identified as Cambisols. Whereas some of the lower terraces showed partly skeletic properties, the soils in the upper parts of the terrace system appear to be more intensively weathered. According to DRIESSEN et al. (2001), Cambisols are characterised by incipient soil formation and beginning differentiation into an A, B and C horizon, which is evident e.g. from changes in colour and structure. There is no evidence of appreciable illuviation of materials like clay, organic matter, aluminium and/or iron compounds. The soils of this group are particularly well represented in temperate and boreal regions that were under the influence of glaciation during the Pleistocene, partly because the soil's parent material is still young but also because soil formation is comparatively slow in cool, northern regions. Erosion and deposition cycles account for the widespread occurrence of Cambisols in mountain regions.

However, the WRB classification – like many profile-based systems - takes insufficient account of the polygenetic structure of the solum. Polygenesis was detected on the main terrace, T7, and for all terraces upslope. This shows that during the formation of the terrace system, soil development was interrupted several times. Besides the continuous and low intensity slope processes, sediment might have been deposited during or immediately after high intensity events such as earthquakes or glacial lake outbursts. Periglacial processes during colder periods resulted in solifluction layers and the deposition of aeolian material.

4.3 Radiocarbon dating

Table 3 summarises the AMS ^{14}C dating results and their interpretation. Translocation of organic material is an important process in the soils of this part of Bhutan (BAILLIE et al. 2003), so that younger C-containing material can infiltrate the sampled horizons from the overlying A horizon(s). The ages therefore represent the minima for the main phases of pedogenesis and are underestimates for the ages of the parent materials.

LEHMKUHL & HASELEIN (2000) mention three major intervals of Holocene soil formation from the neighbouring Tibetan loess plateau (4000-4500 m a.s.l.): 9900-8000 BP, 7400-4600 BP and 3400-2000 BP. This suggests that - compared to our study area - pedogenesis on the Tibetan plateau was interrupted several hundred years earlier each time, which can be explained by the higher elevation of Tibet and the regional variations in monsoonal climate. SAIJO & TANAKA (2002) also mention mid-Holocene (6200-4500 BP) paleosol formation from the Nepalese Thakkhola basin at elevations of 2770-3860 m a.s.l.. Our youngest conventional ^{14}C age for the soil on T10 (1715 ± 25 BP) is in accordance with the findings of IWATA et al. (2002) close to Raphsthreng, northern Bhutan at approximately 4400 m a.s.l.. They dated humic soil materials covered by 0.4 m of moraine material to 1690 ± 40 and 2080 ± 40 ^{14}C years BP.

In addition to our data, GURUNG (2001) reports a ^{14}C measurement for wood remnants found in the gravels of the main river terrace of the Chamkhar Chhu (T7, Fig. 2) near Bathpalathang, 10 km south of our study area. These were dated to 27340 ± 180 years BP. This result is not in contrast to ours as the wood was deposited as part of the alluvial sedimentation, whereas our dating is based on the C_{org} accumulated during post-alluvial pedogenesis. This suggests that the retreat or melting of the source glaciers began earlier than the conventional global LGM (18-25 ka). Furthermore, the well-rounded granite boulders result from long-distance transport and therefore indicate that at this time, the maximum extent of the glaciers was still upstream of the study area. According to geological mapping (GANSSER 1983; DGM 2001), the leucogranites outcrop 50 km north of our study area at approx. 4500 m a.s.l..

Aeolian sediments are missing on all terraces below T7. This suggests that last major loess deposits within the study area occurred in the late Pleistocene or early Holocene and that most of the polygenesis observed results from re-working of local materials (solifluction) during colder Holocene periods.

4.4 Pedogenic indicators of relative dating

Fig. 5 depicts the whole-profile weighted mean particle size distribution for all analysed profiles. As indicated by the grey arrow, a trend from more sandy soils close to the river to more silty/clayey soils on higher terraces is evidenced. There is a significant positive correlation between relative height above the river versus clay+silt ($r^2 = 0.50^{**}$).

Terrace T20, which is 160 m above the current river level does not fit into the general pattern. It is located at the foot of the steepest part of the terrace system (Fig. 2), and has probably received much coarse textured and less weathered material from upslope compared to the other locations examined.

In this context one has to bear in mind that a positive correlation is not necessarily evidence for increasing weathering intensity with increasing relative height above the current river level. Older sediments might have already been finer or “pre-weathered” at the time of their deposition (BÄUMLER 2001b) and therefore significantly influence the results for the profile-weighted means which do not take account of single horizons or genetic units.

The results for the whole-profile weighted means of specific surface area (Fig. 6) of the <2 mm fraction gave a similar pattern. Increasing surface area with increasing terrace level can be taken as another proof for more pronounced weathering upslope. The correlation of the weighted mean clay contents against the surface area measurements produced a highly significant correlation (r^2 = 0,96***).

Besides the neo- and transformation of silicate minerals, the transformation of iron components is a good indicator for pedogenesis. During weathering, iron is released, oxidised and – after some time as poorly crystallised oxidic compounds – finally transformed into well-crystallised Fe compounds. In our study area, the percentage of silicate-bound iron steadily decreases with increasing elevation above the river, whereas well-crystallised iron oxides (Fe_{d-o}) increase (Fig. 7). There are almost constant Fe_o values over time, which indicates that we observe a state of equilibrium between the rate of Fe release from silicate weathering, the formation of Fe_o and the subsequent crystallisation to Fe_{d-o}.

Additionally, the weathering index based on iron oxides, Fe_{d-o}/Fe_t, is given in Fig. 8. It shows a continuous increase from less weathered sites in the lower part of the terrace system to more strongly weathered terraces upslope. Terraces T12 and T20 do not follow the general trend, which was also observed in case of the particle size distribution (Fig. 5).

Other elements can also be used to trace the course of weathering. PARKER's (1970) weathering index uses the unequal release and leaching of sodium, potassium, calcium and magnesium during weathering. Fig. 9 shows that the lower terraces have the highest values (= least weathering), but the increase with age is irregular.

XRD analyses of the clay fractions also indicate the trend and intensity of soil development within the terrace system (Fig. 10). The dominant mineral is kaolinite, which is sharply peaked in all samples, including that from the lowest of the sampled terraces. Some of the kaolinite is presumably inherited from the alluvium and is not all produced by in situ weathering, at least at the lower sites.

The alteration of illite to interstratified minerals and to hydroxy-Al interlayered minerals and pedogenic chlorite with increasing height above the current river can be seen. The ordinate values can also be taken as a measure for the degree of crystallisation and therefore relative age.

All of the profile-weighted parameters show distinctive, more or less “smooth” trends when plotted against increasing relative height above the current river level. This outcome was not necessarily expected, especially when we take into account the different genesis of the two main sections of the Thangbi river terrace system: the sediments of the lower terraces (T1-T6) are younger than 27340 years BP; and no paleosols were detected, indicating that the soils have developed in moderately steep terrain without major interruptions until the present. In contrast, the valley structures of terraces T8 and above existed before late Pleistocene and were repeatedly disturbed by periglacial processes, which were accentuated by the comparatively steep slopes.

The clarity of the trends also indicates that tectonic movements within the valley structure, which could have lead to “offsets” or even reversals, seem unlikely to have occurred since late Pleistocene. However, this does not exclude the moderate regional uplift, as mentioned by BAILLIE & NORBU (2003).

5. Conclusions

Our study provided insight into basic properties of soils regarded as typical for the inner valleys of central Bhutan. Field observations and geomorphological analyses helped to build a preliminary chronology of events. Wood remnants in the sediments of the main terrace, T7 at 41 m above the current river level, were dated to 27340 ± 180 years BP by GURUNG (2001). If we assume that this massive sediment load represents the sediments accumulated towards the end of the last glaciation, it suggests that the last local maximum glaciation may have predated the global LGM. This accords with new findings from eastern Nepal (BÄUMLER 2003).

The same assumption makes all of the terraces above T7 of middle or late Pleistocene age. They can be clearly distinguished from the members of the lower part by their deeper profiles and higher contents of silt and clay indicating that they are more strongly weathered. Furthermore, they show polygenetic structures, which means that soil development was interrupted several times by periglacial phenomena under cold and dry conditions. As no aeolian material was detected below T7 (= 27340 years BP), the interruptions identified at 10175, 8710, 4055 and 1715 years BP represent solifluction events, rather than deposition of fresh loess.

The terraces below T7 are of late Pleistocene and Holocene age. No polygenetic features can be found which indicates that “catastrophic floods” did not occur during this period, and that the Chamkhar Chhu cut into the valley fill by continuous vertical erosion.

The trends we identified in the determination of relative age by particle size distribution, surface area, clay mineral development and weathering indices do not show a distinctive “gap” between the two parts of the terrace system. Even *within* the upper part, relative age increased with increasing level of the terrace. This might be evidence that during the formation of the soils we observe today, in-situ weathering played an important role, reinforcing the possible pre-weathering of aeolian sediments.

The Thangbi terrace system can be regarded as a chronosequence of fluvial sediments and their associated pedal structures. Its vertical amplitude of nearly 300 m makes it comparable with others in the Himalayas, which include many of the biggest river terrace systems in the world.

Acknowledgements

We are deeply indebted to the Bhutanese Ministry of Agriculture (Thimphu), the members of the National Soil Services Centre (Simtokha) and the Soil and Plant Analytical Laboratory (SPAL) for their friendly and professional support.

Without the help from the RNR-RC in Bathpalathang (Jakhar) and the understanding and hospitality of the people of Thangbi the fieldwork would not have been possible.

This work was financed by the Deutsche Forschungsgemeinschaft (DFG), project no. BA 1637/1-2.

References

ARDUINO, E., BARBERIS, E., CARRARO, F. & FORMER, M.G. (1984): Estimating relative ages from iron-oxide/total-iron ratios of soils in the western Po Valley, Italy. – Geoderma **33:** 39-52.

ARDUINO, E., BARBERIS, E., AJMONE MARSAN, F., ZANINI, E. & FRANCHINI, M. (1986): Iron oxides and clay minerals within profiles as indicators of soil age in northern Italy. – Geoderma **37:** 45-55.

BÄUMLER, R. (2001a): Vergleichende bodenkundliche Untersuchungen in Hochasien und Kamtschatka - Böden als Zeugen der quartären Landschafts- und Klimageschichte. – Relief, Boden, Paläoklima **16**, Bornträger, Berlin & Stuttgart, 217 pp.

BÄUMLER, R. (2001b): Pedogenic studies in aeolian deposits in the high mountain area of eastern Nepal. – Quat. Int. **76/77:** 93-102.

BÄUMLER, R. (2003): Pedogenic studies in eastern Nepal – new aspects about the last glaciation. – Quat. Sci. Rev. (submitted).

BAILLIE, I.C., TSHERING, K., DORJI, T., TAMANG, H.B., DORJI, T., NORBU, CH., HUTCHEON, A.A. & BAEUMLER, R. (2003): Regolith and soils in Bhutan, eastern Himalayas. – Eur. J. Soil Sci. (in press).

BAILLIE, I.C. & NORBU, CH. (2003): Climate and other factors in the development of river and interfluve profiles in Bhutan, eastern Himalayas. – J. Asian Earth Sci. (in press).

BHARGAVA, O.N. (ED.) (1995): The Bhutan Himalaya: a geological account. – Geological Survey of India, Special publication **39**, Calcutta, 245 pp.

BHUTAN SOIL SURVEY (1998): Technical Report on the detailed soil survey of Jakhar RNR Research Centre site, Bathpalathang farm. – Report No. **2(a)**, September 1998, 73 pp.

BRUNAUER, S., EMMETT, P. & TELLER, E. (1938): Adsorption of gases in multimolecular layers. – J. Am. Chem. Soc. **60:** 309-319.

DGM (2001): Geological map of Bhutan and neighbouring area (1:1000 000). – Department of Geology and Mines, Ministry of Trade and Industry, Thimphu.

DRIESSEN, P., DECKERS, J., SPAARGAREN, O. & NACHTERGAELE, F. (EDS.) (2001): Lecture Notes on the Major Soils of the World. – World Soil Resources Reports Nr. **94**, FAO, Rome, 334 pp.

FAO (1990): Guidelines for soil description. – Food and Agriculture Organization of the United Nations, Rome, 70 pp.

GANSSER, A. (1983): Geology of the Bhutan Himalaya. – Denkschriften der Schweizerischen Naturforschenden Gesellschaft, Vol **96**, Birkhaeuser, Basel, 181 pp.

GURUNG, D.R. (2001): Quaternary system in the Chamkhar and Tang Valley floor, Bumthang. – Bhutan Geology Newsletter No. **4:** 1-6, Department of Geology and Mines, Royal Government of Bhutan, Thimphu, June 2001.

IWATA, S., NARAMA, C. & KARMA (2002): Three Holocene and late Pleistocene glacial stages inferred from moraines in the Lingshi and Thanza village areas, Bhutan. – Quat. Int. **97/98:** 69-78.

KARAN, P.P. (1967): Bhutan, A Physical and Cultural Geography. – University of Kentucky Press, Lexington, 103 pp.

LEHMKUHL, F. & HASELEIN, F. (2000): Quaternary paleoenvironmental change on the Tibetan Plateau and adjacent areas (Western China and Western Mongolia). – Quat. Int. **65/66:** 121-145.

MEHRA, O.P. & JACKSON, M.L. (1960): Iron oxide removal from soils and clays by dithionite-citrate systems buffered with sodium bicarbonate. – Clays Clay Miner. **7:** 317-327.

MUNSELL, A.H. (1994): Munsell Soil Color Charts. – Revised Edition, MacBeth Division of Kollmorgen Instruments Corp., New Windsor.

NORBU, CH., BAILLIE, I.C., DORJI, TSHERING, DORJI, TSHETEN, TAMANG, H.B., TSHERING, K. & HUTCHEON, A.A. (2003): A provisional physiographic zonation of Bhutan. – J. Bhutan Stud. (submitted).

OKAZAKI, M. (1987): Soils of the Bhutan Himalaya. – in: Life Zone Ecology of the Bhutan Himalaya (ed. M. Ohsawa), Laboratory of Ecology, Chiba University, Tokyo: 145-184.

PAL, D. & SRIVASTAVA, R.A.K. (1982): Landform configuration of the Karewa floor and its implications on the Quaternary sedimentation – Kashmir Valley. – in: Himalaya - landforms and processes (eds. V.K. Verma and P.S. Saklani), Today & Tomorrow Publications, New Delhi, 166 pp.

PARKER, A. (1970): An index of weathering for silicate rocks. – Geol. Mag. **107:** 501-504.

PRASAD,C. & VERMA, V.K. (1974): A study of Quaternary sediments around Asan Valley, Dehradun. – Him. Geol. **4:** 361-370.

RGOB (1994): A geography of Bhutan. Our Natural Environment. – Course book for class VII, 2nd Edition; Education Division, Ministry for Health and Education, Royal Government of Bhutan, Thimphu, 82 pp.

SAIJO, K. & TANAKA, S. (2002): Paleosols of middle Holocene age in the Thakkhola basin, central Nepal, and their paleoclimatic significance. – J. Asian Earth Sci. **21:** 323-329.

SCHWERTMANN, U. (1964): Differenzierung der Eisenoxide des Bodens durch Extraktion mit saurer Ammoniumoxalat-Lösung. – Z. Pflanzenernähr. Düng. Bodenkd. **105:** 194-202.

STUIVER M. & POLACH H.A. (1977): Reporting of C14-data - discussion. – Radiocarbon **19(3)**: 355-363.

SURVEY OF BHUTAN (1999): Topographic map of Trongsa/Bumthang, 1:50000. – Survey of Bhutan, Thimphu.

TAKADA, M. (1991): Landform and Quaternary geohistory of the Bhutan Himalaya. – in: Life Zone Ecology of the Bhutan Himalaya (ed. M. Ohsawa), Laboratory of Ecology, Chiba University, Tokyo: 41-88.

TRÜBY, P. & ALDINGER, E. (1989): Eine Methode zur Bestimmung austauschbarer Kationen in Waldböden. – Z. Pflanzenernähr. Bodenkd. **152:** 301-306.

WINKLER, M.G. & WANG P.H. (1993): Late-Quaternary vegetation and climate of China. – in: Kutzbach et al.: Global Climates Since the Last Glacial Maximum, University of Minnesota Press, Minneapolis: 221-264.

WRB (1998): World Reference Base for Soil Resources. – ISSS, ISRIC, FAO; World Soil Resources Reports **84**, Rome, 90 pp.

YAMANAKA, H., YOSHIDA, M. & ARRITA, K. (1982): Terrace landforms and Quaternary deposits around Pokhara Valley, Central Nepal. – J. Nepal Geol. Soc. **2:** 113-142.

YOSHIDA, M. & IGARASHI, Y. (1984): Neogene to Quaternary lacustrine sediments in the Kathmandu Valley, Nepal. – J. Nepal Geol. Soc. **4:** 73-100.

ZHISHENG, A., PORTER, S.C., ZHOU, W., YANCHOU, L., DONAHUE, D.J., HEAD, M.J., XIHUO, W., JIANZHANG, R. & HONGBO, Z. (1993): Episode of Strengthened Summer Monsoon Climate of Younger Dryas age on the Loess Plateau of Central China. – Quat. Res. **39:** 45-54.

ZHOU, W., DONAHUE D.J., PORTER, S.C., JULL, T.A., XIAOQIANG L., STUIVER M., ZHISHENG A., MATSUMOTO E. & GUANGRONG D. (1996): Variability of Monsoon Climate in East Asia at the End of the Last Glaciation. – Quat. Res. **46:** 219-229.

ZÖLLER, L (2000): Chronology of upper Pleistocene 'red silts' in the Siwalik system and constraints for the timing of the upper Palaeolithic in Nepal. – Catena **41:** 229-235.

Table 1: Profile descriptions of terraces T4 and T19.

T4, lower terrace soil (27 m terrace) 27°37'N, 90°42'E; 2682 m; arable (wheat) Endoskeleti-eutric Cambisol (WRB, 1998)		T19 upper terrace soil (153 m terrace) 27°36'N, 90°42'E; 2808 m; pasture (cattle) Hapli-eutric Cambisol (WRB, 1998)	
0-16 cm (A)	10YR 3/3; sandy loam; subangular to platy; slightly moist; few fine pores; common fine roots; granite gravels, many well-rounded, partly weathered boulders throughout the whole profile; diffuse boundary	0-20 cm (A)	10YR 3/4; clay loam, probably aeolian sediment; friable consistence; almost dry; common fine pores; common medium and fine roots; no stones; diffuse boundary
16-28 (B1)	10YR 4/3; sandy loam; subangular; almost dry; few fine pores; few fine roots; frequent quartz stones; diffuse boundary	20-47 (B1)	10YR 4/4; sandy loam, probably aeolian sediment; subangular blocky; almost dry; common fine pores; few medium and fine roots; no stones; diffuse boundary
28-39 (B2)	10YR 3/4; sandy loam; subangular; almost dry; few fine pores; very few fine roots; few quartzitic gravels; clear wavy boundary	47-118 (2B2)	2.5Y 5/4; sandy loam, probably solifluction layer; subangular to platy; almost dry; few fine pores; very few fine and medium roots; few stones from granite, gneiss, quartzite and amphibolite; diffuse boundary
39-64 (CB)	2.5Y 6/3; sand; single grain structure; almost dry; few fine pores; very few fine roots; granitic gneiss; clear wavy boundary	118-190 (2B3)	10YR 5/4; sandy clay loam; subangular to platy; almost dry; few fine pores; very few fine roots; very few stones; diffuse boundary
64-90+ (C)	2.5Y 7/4; sand; granitic parent material weathered to single grain structure; almost dry; very few fine pores; no roots	190-230 (2B4)	10YR 4/4; silty loam; subangular to polyhedral; almost dry; common fine pores; no roots; very few stones; diffuse boundary
		230-295 (2B5)	10YR 4/4; sandy clay loam; subangular blocky; almost dry; common fine pores; no roots; very few stones; clear horizontal boundary
		295-305 (3A)	10YR 3/3; silty loam; subangular blocky; clayskins; almost dry; common fine pores; no roots; very few stones; clear horizontal boundary
		305-380 (3Bt)	10YR 5/8; clay loam; subangular to polyhedral; clayskins; almost dry; common fine pores; no roots; very few stones; diffuse boundary
		380+ (3C)	weathered parent material; not sampled

Table 2: Selected analytical data of six typical profiles.

profile/horizon	depth [cm]	bulk density [g cm^{-3}]	$pH_{H2O\,dest.}$	C_{org} [%]	CEC [$cmol_c$ kg^{-1}]	Fe_d [g kg^{-1}]	Fe_o [g kg^{-1}]	Al_d [g kg^{-1}]	Al_o [g kg^{-1}]	sand, silt, clay [%]	surface area [m^2 g^{-1}]
T4, PT036, 27 m above the current river level											
A	0-16	1.28	5.4	1.81	4.80	5.82	3.42	1.15	1.78	54, 22, 24	6.0
B1	16-28	1.24	5.6	1.11	4.49	4.74	3.21	1.23	2.00	53, 24, 23	7.9
B2	28-39	1.23	5.8	0.71	3.32	3.21	2.25	0.99	1.51	67, 19, 14	6.1
BC	39-64	1.33	6.1	0.12	1.14	0.65	0.56	0.28	0.51	88, 6, 6	1.9
C	64-90+	1.28	6.2	0.06	0.48	0.43	0.39	0.22	0.35	90, 4, 6	1.2
T7, PT039, 40 m above the current river level											
A	0-23	-	5.2	2.87	2.90	5.52	3.34	5.04	9.46	46, 35, 19	7.5
2A	23-40	-	5.8	1.74	3.07	3.25	1.55	4.04	7.78	49, 34, 17	8.2
2B	40-57	-	5.8	0.86	1.17	2.31	1.06	2.07	10.20	80, 14, 6	1.8
2CB	57-75	-	5.9	0.48	0.73	1.81	0.61	1.28	8.99	85, 8, 7	1.2
2C	75-100+	-	5.9	0.15	0.40	1.32	0.21	0.62	2.55	89, 5, 6	1.2
T10, PT049, 85 m above the current river level											
A	0-20	0.99	5.4	3.32	4.12	5.44	3.99	4.50	6.86	49, 35, 16	9.3
2A2	20-43	0.96	5.5	2.35	3.37	5.78	4.06	3.96	5.62	49, 30, 21	10.3
2B	43-142	1.26	5.6	0.45	3.00	7.33	4.09	2.18	2.74	48, 30, 22	18.6
3A3	142-185	1.08	5.6	0.91	1.62	8.46	4.68	3.72	5.75	49, 30, 21	18.1
3B	185-230	1.15	6.1	0.18	4.18	7.24	1.90	2.11	1.13	62, 28, 10	16.3
3C	230+	-	6.2	0.12	6.32	8.48	1.93	1.52	1.25	69, 24, 7	15.2
T17, PT043, 136 m above the current river level											
A	0-17	0.83	5.4	3.10	2.47	9.72	4.19	3.81	7.58	50, 30, 20	11.0
B1	17-36	0.92	5.5	1.98	2.54	9.12	4.20	3.53	5.40	49, 32, 19	12.6
2A	36-52	1.06	5.5	1.12	3.34	10.09	4.19	2.49	2.53	50, 29, 21	14.0
2B2	52-95	1.30	5.4	0.60	3.46	9.37	3.90	2.09	1.76	51, 29, 20	13.4
2B3	95-190	1.32	5.5	0.53	3.70	9.64	3.85	2.16	1.73	51, 29, 20	13.9
2C	190-210	-	5.9	0.13	3.92	4.54	0.88	0.86	1.49	81, 12, 7	3.5
T19, PT042, 153 m above the current river level											
A	0-20	0.89	5.5	4.44	6.37	7.30	3.71	4.42	7.57	51, 26, 23	8.4
B1	20-47	0.99	5.7	1.90	2.32	9.49	3.72	3.01	6.09	55, 2, 18	10.7
2B2	47-118	1.34	5.8	0.50	3.31	8.82	4.01	1.38	1.14	53, 26, 21	11.2
2B3	118-190	1.38	5.7	0.47	3.32	12.99	3.69	2.33	1.42	52, 26, 22	16.0
2B4	190-230	1.25	5.3	0.72	3.86	15.47	4.64	3.11	2.53	46, 29, 25	18.7
2B5	230-295	1.07	5.3	1.11	2.51	12.93	5.36	4.66	6.03	42, 32, 26	20.9
3A	295-305	0.94	5.4	2.07	3.80	17.66	9.24	5.23	5.51	27, 35, 38	23.4
3Bt	305-380	0.99	5.4	0.90	3.63	22.48	8.93	4.82	4.61	22, 36, 42	33.6
3C	380+	-	5.4	0.39	2.66	12.88	4.06	2.40	2.03	47, 30, 23	17.8
T28, PT041, 266 m above the current river level											
A	0-62	0.78	5.7	2.31	1.24	18.78	4.53	4.49	11.67	25, 40, 35	35.0
B	62-85	0.95	5.6	1.37	2.72	15.34	5.79	3.47	4.56	28, 42, 30	29.6
C	85-99	0.98	5.8	0.65	1.87	7.70	3.00	1.81	2.35	52, 29, 19	18.7
2C	99-115	1.26	5.9	0.25	1.15	8.10	1.83	1.27	1.32	69, 20, 11	11.0
3A	115-140	0.88	5.8	1.62	2.73	29.62	10.73	6.36	6.33	14, 42, 44	43.9
3B2	140-160	0.97	5.9	0.43	2.92	25.87	3.49	5.69	2.56	19, 38, 43	43.0
3B3	160-220	1.20	6.0	0.25	2.41	14.65	2.49	2.95	1.76	30, 37, 33	33.0
3C	220-265+	1.35	6.1	0.12	1.57	7.03	1.51	2.42	1.18	60, 24, 16	15.8

Table 3: Results and interpretation of AMS ^{14}C dating of selected horizons; conventional age according to STUIVER & POLACH (1977).

terrace	sample	hori-zon	conventional radiocarbon age	interpretation
T19	PT042/8 KIA14502	3Bt	10175 ± 60 BP	soil formed during temperature fluctuations in the Younger Dryas (ZHISHENG et al. 1993, ZHOU et al. 1996)
T28	PT041/6 KIA14503	3B2	8710 ± 55 BP	fairly warm and moist conditions during Early Holocene, but still before the climate optimum (WINKLER & WANG 1993)
T9	PT050/X KIA14500	2B	4055 ± 30 BP	mid to late Holocene cooling period (4000 – 3000 BP); solifluction and distinct redistribution of aeolian sediments all over Central and High Asia (BÄUMLER 2001a)
T10	PT049/4 KIA14501	3A3	1715 ± 25 BP	probably marking another period of temperature fluctuations accompanied by enhanced solifluction during the Subatlantic period (late Holocene)

Addresses of the authors: Thomas Caspari and Rupert Bäumler: Technische Universität München, Lehrstuhl für Bodenkunde, 85350 Freising-Weihenstephan, Germany. – Tshering Dorji, Chencho Norbu and Kado Tshering: National Soil Services Centre, Ministry of Agriculture, Royal Government of Bhutan, PO Box 119, Simtokha, Bhutan. – Ian Baillie: National Soil Resources Institute, Cranfield University, Silsoe, MK45 4DT, England, UK.

Corresponding author: Thomas Caspari, Technische Universität München, Lehrstuhl für Bodenkunde, 85350 Freising-Weihenstephan, Germany. E-mail: caspari@wzw.tum.de

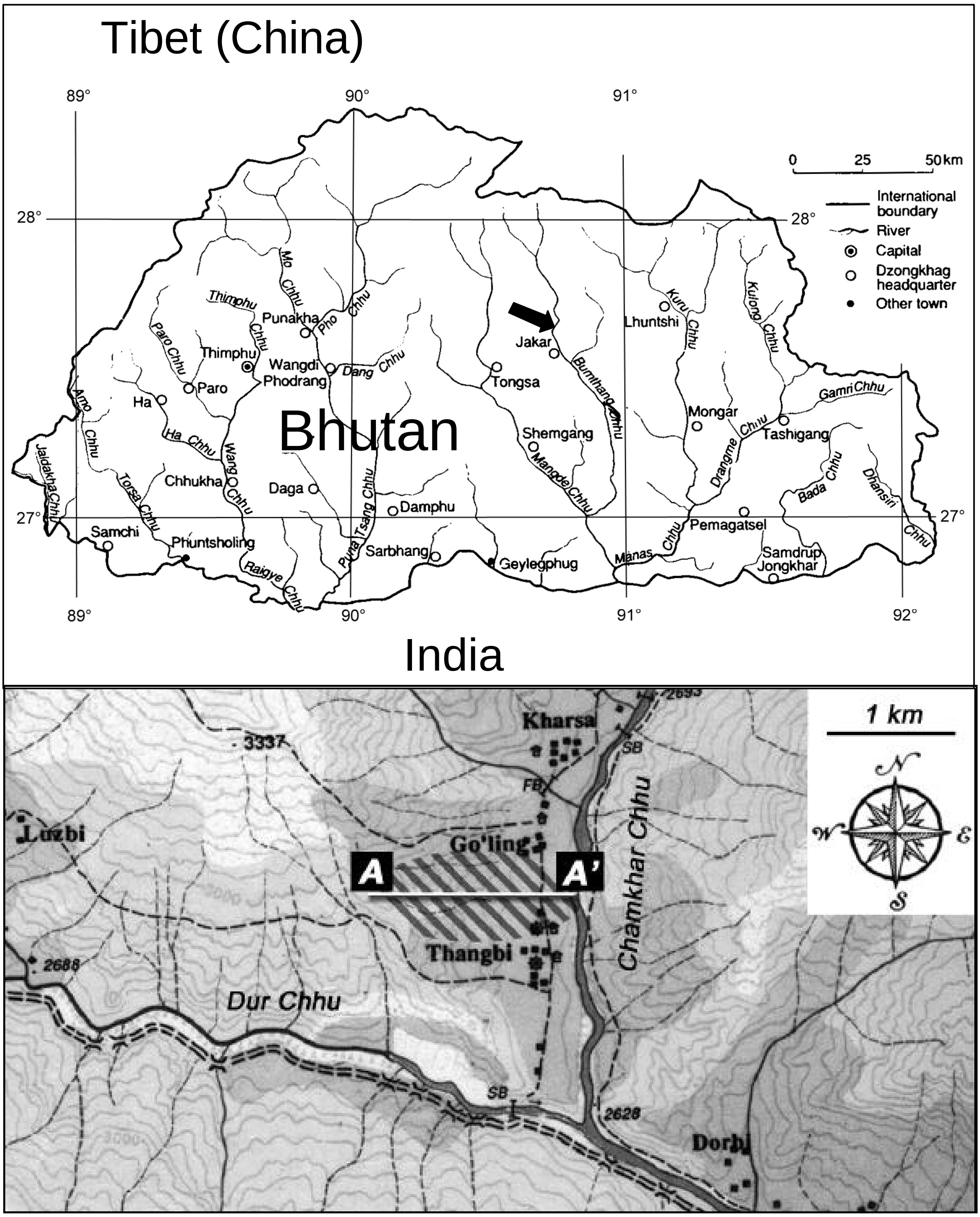

Fig. 1: Location of the Thangbi river terrace system within Bhutan (arrow) and on the topographic map (hatched area); the section A-A' is shown in Fig. 2; after: RGoB (1994, modified) and Topographic Map of Trongsa/Bumthang 1:50000 (Survey of Bhutan 1999).

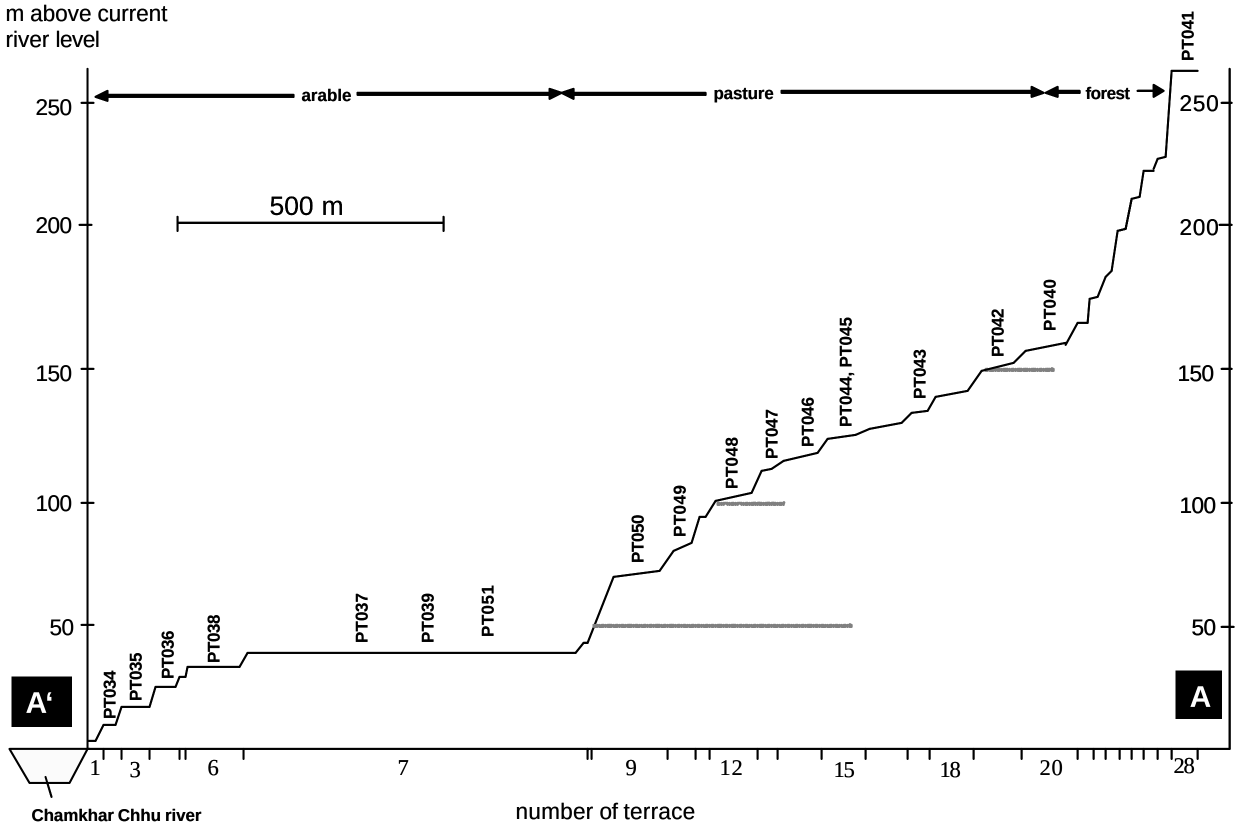

Fig. 2: Section through the Thangbi terrace system from east (A') to west (A); the profile IDs show the approximate location of the soil pits; underlined profiles are covered by loess.

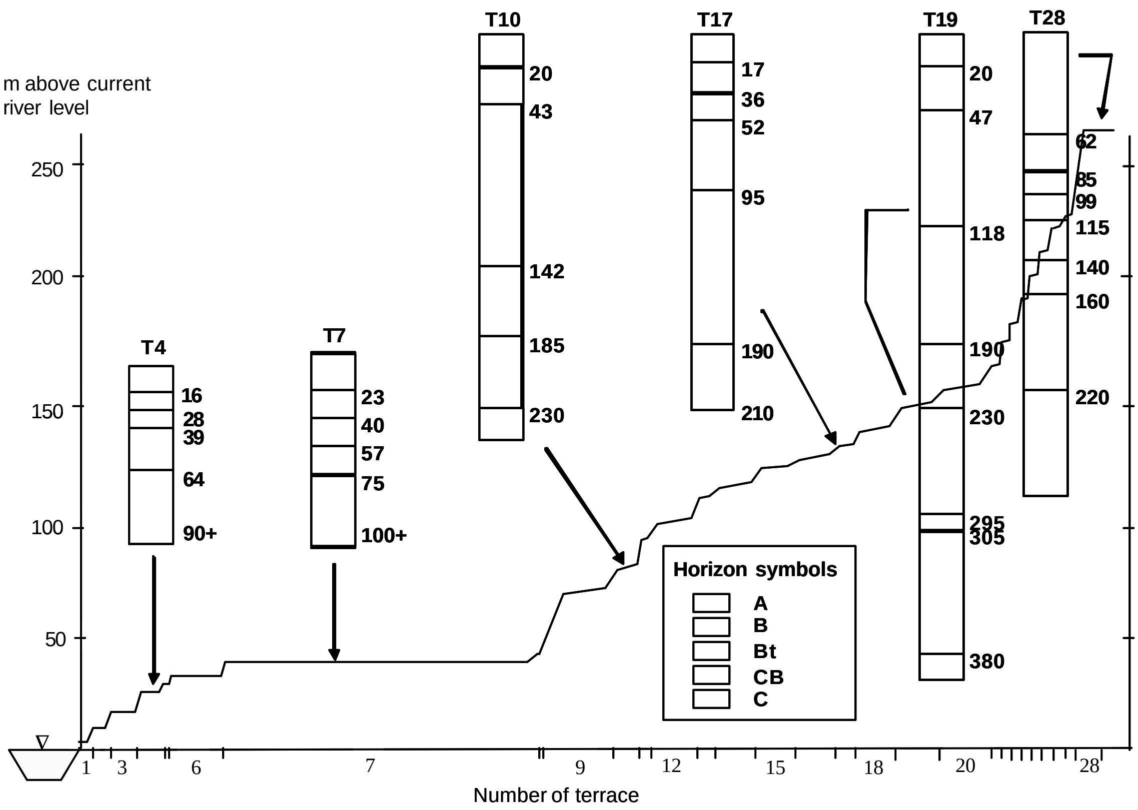

Fig. 3: Selected standard profiles and their horizon designations after WRB (1998); arrows show the location of the sampling sites; numbers indicate horizon boundaries in cm below the surface.

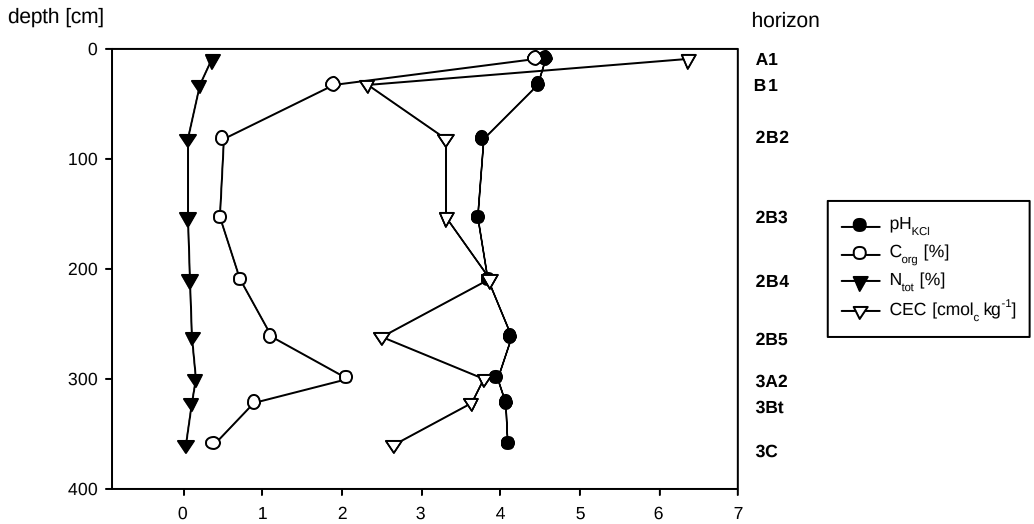

Fig. 4: Gradients of pH_{KCl}, C_{org}, N_{tot} and CEC of profile PT042 (T19).

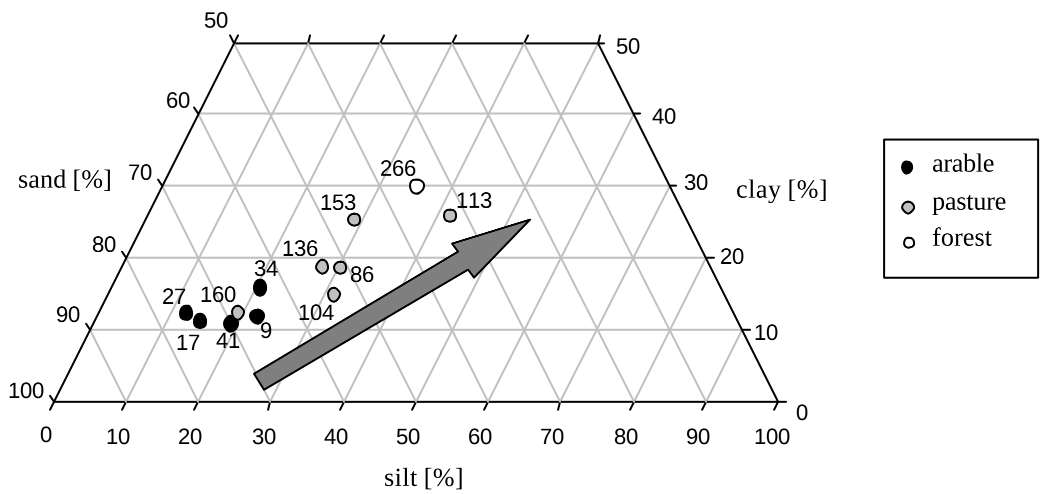

Fig. 5: Ternary diagram showing the whole-profile weighted means of particle size distributions; numbers indicate altitude of the terraces in m above the current river level.

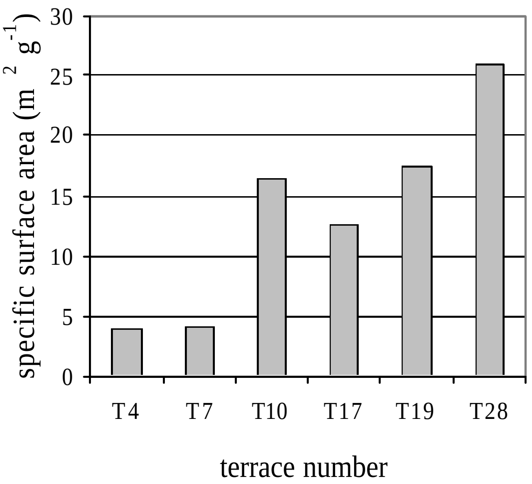

Fig. 6: Whole-profile weighted means of the surface area measurements for selected profiles.

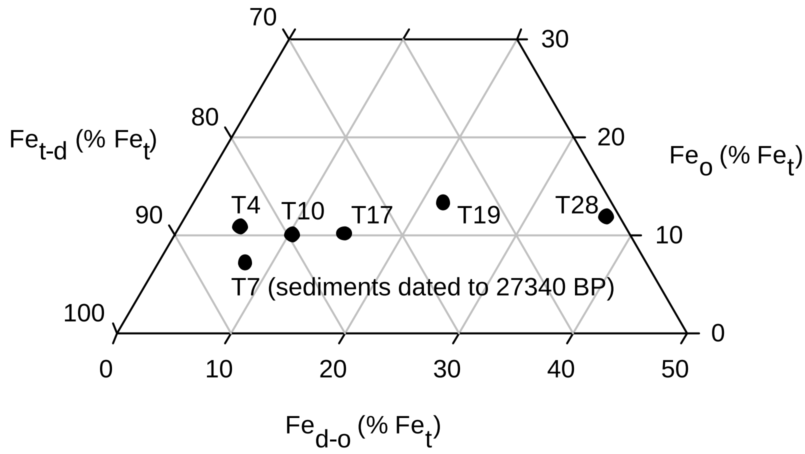

Fig. 7: Whole-profile weighted means of silicate-bond iron (Fe_{t-d}), well-crystallised Fe oxides (Fe_{d-o}) and poorly crystallised oxidic Fe compounds (Fe_o), plotted as percentage of total iron (Fe_t).

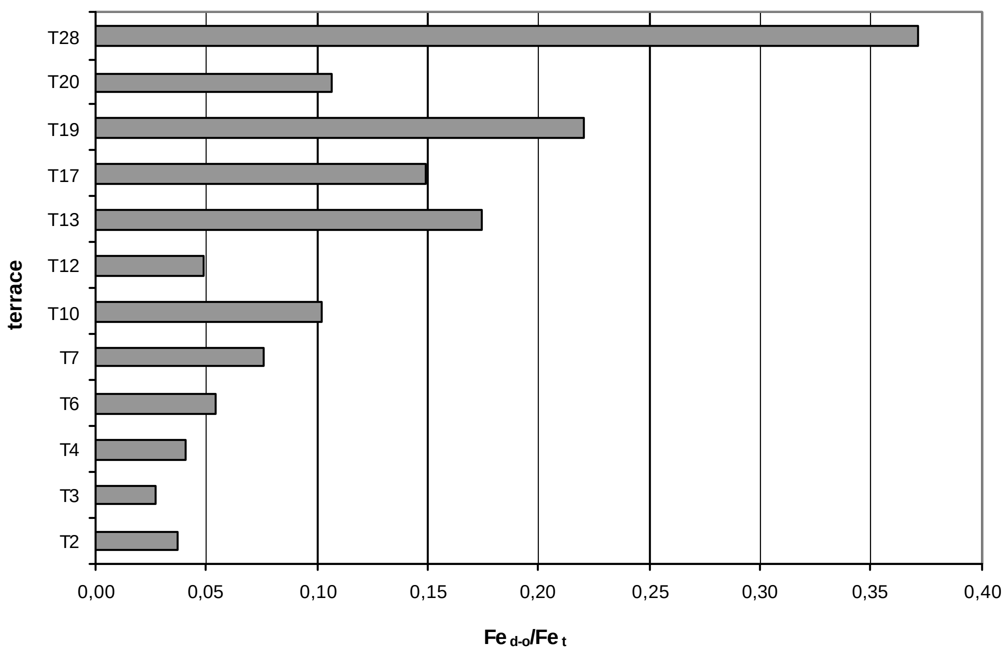

Fig. 8: Ratio of well-crystallised iron oxides (Fe_{d-o}) to total iron content (Fe_t); whole-profile weighted means for all examined terraces.

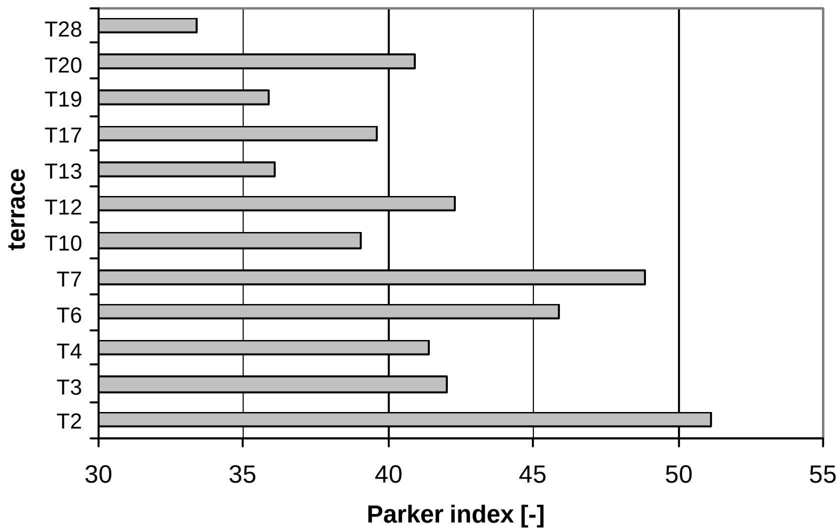

Fig. 9: Whole-profile weighted means of Parker index values.

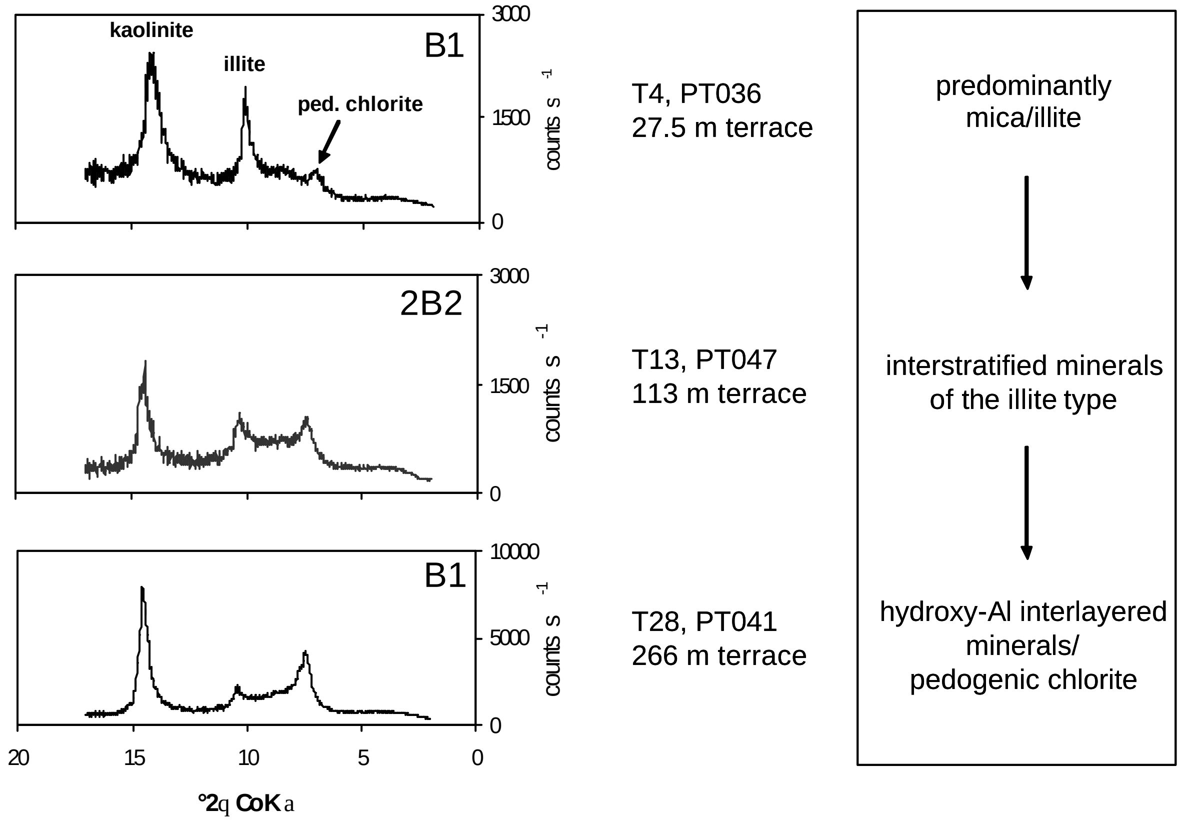

Fig. 10: Comparison of XRD patterns of the Mg-saturated clay fractions; B horizons from terraces T4, T13 and T28.